Removal of organic matters and dyes from aqueous solutions and effluent of a hybrid airlift A2O bioreactor treating milk processing wastewater using chemically derived bituminous-based activated carbons

Rahimi, Zahra; Zinatizadeh, Ali Akbar; Zinadini, Sirus; Younesi, Habibollah; van Loosdrecht, Mark; Azizi, Shohreh

DOI
10.1016/j.jwpe.2025.107015

Publication date
2025

Document Version
Final published version

Published in
Journal of Water Process Engineering

Journal of Water Process Engineering 70 (2025) 107015

Contents lists available at ScienceDirect

Journal of Water Process Engineering

journal homepage: www.elsevier.com/locate/jwpe

Removal of organic matters and dyes from aqueous solutions and effluent of a hybrid airlift A2O bioreactor treating milk processing wastewater using chemically derived bituminous-based activated carbons

Zahra Rahimi [a], Ali Akbar Zinatizadeh [a,b,*], Sirus Zinadini [a], Habibollah Younesi [c], Mark van Loosdrecht [d], Shohreh Azizi [e]

[a] Department of Applied Chemistry, Faculty of Chemistry, Razi University, P.O. Box 67144-14971, Kermanshah, Iran
[b] Australian Centre for Water and Environmental Biotechnology (ACWEB, formerly AWMC), Gehrmann Building, The University of Queensland, St. Lucia, 4072 Brisbane, Australia
[c] Department of Environmental Science, Faculty of Natural Resources and Marine Sciences, Tarbiat Modares University, P.O. Box 46414-356, Noor, Iran
[d] Department of Biotechnology, Delft University of Technology, Julianalaan 67, 2628 BC Delft, the Netherlands
[e] UNESCO-UNISA Africa Chair in Nanosciences and Nanotechnology, College of Graduate Studies, University of South Africa, Muckleneuk Ridge, PO Box 392, Pretoria, South Africa

ARTICLE INFO

Editor: Sadao Araki

Keywords:
Wastewater post-treatment
Residual organic matters
Adsorption process
Activated carbon
Bitumen

ABSTRACT

The synthesis of chemically derived bituminous-based activated carbons (ACs) was conducted in this research. The study examined the efficacy of the KOH-2 modified AC by conducting batch experiments under different operating settings. Pollutant concentration, adsorbent dosage and contact time were considered as variables. Bovine serum albumin (BSA), dextrose, and methylene blue (MB) were used as model substances to represent protein, carbon, and textile dyes, respectively. Under optimal conditions, the activated carbon modified with a 2:1 impregnation ratio using KOH showed the best performance among two other ACs, therefore, that was introduced as chosen AC. The optimal parameters were determined as pollutant concentration, adsorbent dosage and contact time obtained to be 600 mg/L, 0.22 g/L and 220 min; 200 mg/L, 0.6 g/L and 180 min; 200 mg/L, 1 g/L and 196 min for MB, BSA and dextrose, respectively. This AC obtained the highest adsorption capacity of 2710.6, 283, and 273 mg/g adsorbing MB, BSA and dextrose, respectively. In the following, column studies were conducted using biologically treated wastewater obtained from a new one-stage hybrid internal circulation airlift A2O bioreactor to eliminate soluble microbial products (SMP). It was seen that the adsorption column, which was filled with the AC under optimal experimental conditions (bed height of 4.5 cm and solution flow rate of 5 mL/min), resulted in a decrease in residual organic substances from 35 mg-TOC/L to 6.6 mg-TOC/L. It is worth mentioning that the utilization of an integrated approach involving sophisticated biological treatment and post-treatment technology has demonstrated efficacy in the elimination of residual organic substances.

1. Introduction

Biological treatment-based processes are widely and smoothly adopted to wastewater treatment plants (WWTPs) all over the world. Biological processes are environmentally friendly, cost-effective, and provide high performance compared to other technologies, such as physical, chemical, and advanced methods. However, the main challenge of biological treatment is that the effluent from wastewater treatment plants (WWTPs) often contains a variety of soluble organic compounds, commonly referred to as soluble microbial products (SMPs). Since the bioreactors are often implemented under non steady state conditions due to the inevitable variations in feed flow rate and composition. It is documented even if the bioreactor can be regarded in steady state conditions, the microorganisms grow under dynamic conditions in various zones of the bioreactor. SMP possesses organic characteristics released through bacterial secretion during biological treatment. The SMPs are mainly including proteins, carbohydrates and humic-like substances. Nonetheless, it is noted the proteins and carbohydrates are known as main constituents of the bioreactors' effluent. The existence of such compounds in the treated wastewater influences

* Corresponding author at: Department of Applied Chemistry, Faculty of Chemistry, Razi University, P.O. Box 67144-14971, Kermanshah, Iran.
E-mail address: zinatizadeh@razi.ac.ir (A.A. Zinatizadeh).

https://doi.org/10.1016/j.jwpe.2025.107015
Received 14 October 2024; Received in revised form 27 December 2024; Accepted 14 January 2025
Available online 17 January 2025

severely following post-treatment processes, discharge level of the effluent, environmental implications and water reuse issue.

Another common pollutant that has extremely restricted the use of the treated wastewaters is dye molecules that are extremely water-soluble and discharged from various industrial sections [1]. These pollutants are stable and fastness against degradation, and cause numerous injurious complications on the human health like cancer, allergy, skin irritation, and toxicity. Taking into consideration these sever health hazards, the employment of supplemental treatment for the biologically treated wastewaters containing SMP and dyes is urgently required for more widespread application of the wastewater treatment plants' effluent.

In general, some popular technologies applied to remove the inorganic and organic pollutants from aqueous environment are including flocculation, electrocoagulation process, membrane-based filtration, adsorption processes, and photocatalytic degradation. Although membrane technology, utilizing filtration and adsorption mechanisms, has achieved up to 98.6 % removal of methylene blue (MB) from wastewater [2], fouling phenomenon has limited the widespread application of such advanced technologies. Photocatalytic degradation can be considered a fast and time-saving technology; however, the synthesis of photocatalysts is expensive, complex, and time-consuming. The significant production of sludge and the formation of large particles in the coagulation/flocculation process pose considerable challenges [3,4]. The advantages and disadvantages of various technologies can be found in the literature [4]. Of these methods, the adsorption processes are more effective and efficient to remove dyes and other pollutants [5]. More importantly, the adsorption processes is a clean technology to some extent, and don't produce the sludge like coagulation-assisted treatment methods [6]. Regarding the various adsorbents, the porous carbon entitled activated carbon (AC) is known as the preferred adsorbent owing to benefiting from distinguishing structural characteristics i.e. the large surface area, porous structure, the abundant functional groups and high surface reactivity [7,8]. Nowadays, the increase in introduction of varied pollutants and their discharge into the water sources and the strict environmental regulations led to the increase in the demand of the AC production. Coal, agricultural wastes, industrial reminds and lignite are commonly employed as potential precursors to synthesize the activated carbon [9]. As an example, pore size distribution of commercial granular activated carbons (GAC) produced from bituminous, coconut, and lignite on removal of the methyl tertbutyl ether (MTBE) from water at ppb concentrations and the absence of natural organic matter (NOM) was surveyed [10]. In this study, the parent activated carbons provided commercially were tailored using thermal and gas treatment. The methylene blue (MB) molecules with 700 mg/L concentration were successfully removed (99.95 %, 350 mg/g) from aqueous solution using 2 g/L of cork-based AC with size of 30–50 μm [11]. In this study, according to the heterogeneity factor ($n > 1$), the physical adsorption mechanism was favorable. The favorable AC was activated by partial replacement of alkaline wastewater with commercial NaOH as activator (50:50 Vol%) after 5 min. Kumar et al. obtained an efficient activated carbon with enhanced structural features (large surface area of 2869 m^2/g and high pore volume of 1.96 cm^3/g) to remove organic pollutants (MB and phenol) from aqueous media. The adsorption of MB occurred through three primary mechanisms i.e. electrostatic interaction, dispersive interaction, and pore size distribution or molecular sieving. Nonetheless, chemical activator used in this study ($ZnCl_2$) was not environmentally friendly caused health and environmental risks [5]. Also, Wang et al., fabricated an activated carbon from sodium carboxymethyl cellulose as a green feedstock with chemical activator of $ZnCl_2$ for dye removal from the water [12]. The high surface area (2429.76 m^2/g) and the nature of various tested dyes (methyl violet, allura red and congo red) influenced on the adsorption capacity. The adsorption process was adopted by double layer adsorption model. Also, commercial bituminous-based GAC tailored with the ZrO_2 nanoparticles removed simultaneously arsenic and methylene blue from water related to the enhanced surface area and ZrO_2 accessibility compared to tailored lignite-based GAC [13]. The MB adsorption was controlled by pore size distribution, the size of hydrated MB molecule, and physical blockage of AC surface in the macro-pore range. This study revealed the proper selection of the GAC influences on the adsorption capacity. The commercial GACs with different sources (bituminous, lignite and wood) were tailored by iron via various protocols (oxidation using various oxidants, precipitation and evaporation) to remove arsenic from ground water over continuous experiments [6]. From the results, the GACs preloaded with iron using precipitation and evaporation showed the breakthrough volume bed of 25,000–34,000 BV with effluent concentrations of 10 ppb. The adsorptive microcrystalline nanocellulose-based nanofiltration membrane exhibited a chemisorption mechanism when tested with methylene blue (MB) as the adsorbate [14].

Based on literature review, this study was the first report regarding the removal of residual COD and SMP from effluent of a one-single hybrid dual internal circulation airlift A2O (DCAL-A2O) bioreactor treating milk processing wastewater (MPW) using activated carbons (AC) chemically synthesized from bituminous-based coal [15]. In addition, the function of the synthesized ACs in adsorption of MB from aqueous solutions was studied. It is worth noting that Iran has abundant bituminous- coal-based mines that currently lack significant applications. Utilizing bitumen as waste for the production of activated carbon offers a valuable way to create an added-value product. Specifically, the precursors of existing commercial activated carbons are being depleted, making bitumen a promising alternative. Consequently, employing bitumen as a low-cost precursor can substantially lower operational costs and mitigate the environmental impact associated with the removal of residual organic matter and dyes from wastewater.

2. Experimental

2.1. Demineralization and pre-oxidation of the bituminous-based coal

In this study, bituminous-based coal received from a mine located in Kermanshah, Iran was employed as precursor to synthesize the activated carbon. To get the favorable size of precursor (150–250 μm), the coal was crushed and sieved. Then, demineralization process was conducted over treatment of precursor with HCl (20 %) and HF (25 %) to remove the interference of the ash [16]. To get this purpose, firstly the raw coal and the aqueous solution of HCl (20 %) were stirred continuously at 60 °C for 2 h. The choline ions were removed from the mixture over filtration and successive washing with hot distilled water. Afterwards, the same procedure was repeated with aqueous solution of HF (25 %) to complete the demineralization process. Finally, the demineralized and acid-treated coal was air-dried at 110 °C and maintained in a desiccator. In continuation, the pre-oxidation process was conducted on the demineralized coal in a muffle furnace under air at 573 K for 12 h. Further, the demineralization process was repeated for the pre-oxidized coal according to the same procedure described for the raw coal. The proximate analysis was carried out for the raw coal, the demineralized raw coal, the pre-oxidized raw coal, the demineralized acid-treated coal, and acid-treated demineralization coal.

2.2. Activated carbon synthesis

The activated carbon-based adsorbents were chemically manufactured using pre-oxidized bituminous-based coal then acid treated (the pre-oxidized demineralized coal) as precursor using KOH, K_2CO_3 and H_3PO_4 as chemical activators over a one-step process [31]. The modified precursor was impregnated with chemical activator at various weight ratios (1:1, 2:1 and 3:1) and mixed for 24 h. Then, the impregnated components air-dried in an oven (at 110 °C for 24 h) were placed in a tubular furnace at activation temperature and time of 800 °C and 1 h, respectively. The heating rate and N_2 gas flow rate were adjusted at 5 °C/min and of 200 mL/min, respectively. Next, any impurities were

removed from the synthesized activated carbons over successive washing with hot and cold distilled water until the neutral pH. Eventually, the final ACs were obtained after being dried in an oven at 110 °C for 24 h.

2.3. Reagents and analytical methods

Methylene blue (MB), bovine serum albumin (BSA) and dextrose as adsorbate were purchased from Merck Company, Germany. These adsorbates were employed as models dye, protein and carbohydrate [17], respectively, to evaluate the capacity of the activated carbons in removing textile dyes and residual COD as SMP from the wastewater treatment plants. To treatment of precursor, HCl (37 %) and HF (40 %) were provided from Merck Compamy, Germany. Chemical activators of KOH (>99 %), K_2CO_3 (>99 %) and H_3PO_4 (85 %) were purchased from Merck company, Germany.

The MB concentration was obtained spectrophotochemically by UV–Visible spectrophotometer. To determine the contents of protein and carbohydrate of SMP, the Lowry and the phenol-sulfuric acid methods, respectively, were followed [18,19]. The TOC amounts were detected through the combustion- infrared method using a TOC analyzer (TOC-5000A, Shimadzu).

2.4. Characterization of precursor and synthesized activated carbons

Fourier Transform Infrared (FTIR) spectroscope (FTIR – AVATAR 370, Thermo Nicolet) was employed to characterize the functional groups. For investigation of the thermal behavior of the raw bituminous-based coal, TGA/DTA analysis was recorded by a Pyris Diamond Thermogravimetric analyzer (PerkinElmer, UK). The textural characteristics of the activated carbon including specific surface area (S_{BET}), micro- and meso-porosity, were determined through N_2 adsorption/desorption tests at 120 °C (Micromeritics ASAP 2010). Scanning electron microscopy (SEM) images were taken to study the surface morphology of the synthesized activated carbons (ProX, Phenom, Netherland). Before SEM imaging, in order to enhance visibility of the surface morphology, the activated carbon samples were covered with gold.

2.5. Batch adsorption experiments

Initially, the preliminary experiments were conducted as batch wise to determine the optimum activated carbon among three various sets of the activated carbons synthesized using three chemical activators i.e. KOH, K_2CO_3 and H_3PO_4 with impregnation ratios of 1:1, 2:1 and 3:1, and dosage of 0.2 g/L from each adsorbent and 100 mL of MB solution with initial concentration of 600 mg/L. The adsorption experiments were done at contact time and agitation speed of 3 h and 200 rpm, respectively, under ambient temperature without setting pH. The KOH-2 impregnated AC (2:1) revealed the uppermost function (as dye removal and adsorption capacity) over the others. In the following, batch experiments were conducted to screen the activated carbons impregnated with KOH and determine the optimum activated carbon using two other adsorbates namely bovine serum albumin (BSA) and dextrose as model protein and carbohydrate, respectively. Accordingly, the functionality of the synthesized activated carbons impregnated with varied ratios of KOH to precursor as 1:1, 2:1 and 3:1 was investigated in a set of six erlenmeyers using 100 mL of BSA and dextrose with initial concentration of 200 mg/L, 0.5 g/L of each adsorbent, contact time and agitation speed of 3 h and 200 rpm, respectively, under ambient temperature without setting pH. The activated carbon impregnated with ratio of 2:1 was recognized as the optimum activated carbon to conduct the rest of the batch adsorption experiments. Using spectrophotometric approaches and employing the Lowry and the phenol-sulfuric acid methods, the extents of protein and carbohydrate, respectively, were analyzed [18,19]. The absorbance of MB, BSA and dextrose adsorbates upon the adsorption process were measured using UV–Visible spectrophotometer at λ_{max} of 664, 750 and 490 nm, respectively. The function of KOH-2 impregnated activated carbon as a chosen adsorbent was then optimized as adsorbent dosage, initial adsorbate concentration and contact time for three adsorbates (MB, BSA and dextrose) at constant agitation speed of 200 rpm under ambient temperature without setting pH over batch adsorption experiments described in the following [20].

To study the impact of initial adsorbate concentration, the batch experiments were accomplished at various initial concentrations of adsorbates as the MB (300, 400, 500, 600, 700, 900 & 1000 mg/L), BSA (100, 200 & 300 mg/L) and dextrose (100, 200 & 300 mg/L) at constant adsorbent dosage (0.2, 0.5 and 0.5 g/L for MB, BSA and dextrose, respectively), contact time (3 h) and agitation speed (200 rpm). To get optimal dosages of adsorbent, adsorption function of KOH-2 impregnated AC was checked at 0.1–1.0 g/L, 0.2–1.0 g/L and 0.5–1.5 g/L for MB, BSA and dextrose, respectively, at optimum initial concentration of adsorabates and other variables considered to be constant (contact time of 3 h and agitation speed of 200 rpm). In the following, the contact time was optimized for each adsorbate at the optimal values obtained for various parameters (initial concentration and adsorbent dosage). In each optimizing step, the function of the chosen AC (KOH-2 AC) was evaluated as the removal efficiency (R, %) and the adsorption capacity using the following equations [21]. To be noted, the adsorption capacity was determined at equilibrium state (q_e, mg/g) and time t (q_t, mg/g).

$$R\ (\%) = \frac{(C_0 - C_e)}{C_0} \times 100 \tag{1}$$

$$q_{e/t}(mg/g) = \frac{(C_0 - C_e) \times V}{M} \tag{2}$$

here, C_0 and C_e are defined as the initial and equilibrium concentrations of various adsorbates (mg/L), respectively. V and M refer to solution volume (L) and adsorbent dosage (g), respectively.

2.6. Adsorption kinetic and isotherm studies

In this section, the experimental data were fitted with popular models to examine the kinetics and isotherms. For finding the controlling mechanism of the adsorption process, intra-particle diffusion model was employed (Eq. (3)) [22].

$$q_t = K_p t^{0.5} + C \tag{3}$$

here, q_t, K_p, $t^{0.5}$ and C are representative of the adsorption capacity (mg/g) at time t (min), rate constant (mg/g $min^{1/2}$), half-time ($min^{0.5}$) and the intercept, respectively. To study kinetics of the adsorption process, the pseudo-first order (Eq. (4)) and the pseudo-second order (Eq. (5)) models commonly used were employed [23,24].

$$ln(q_e - q_t) = lnq_e - k_1 t \tag{4}$$

$$\frac{t}{q_t} = \frac{1}{k_2 q_e^2} + \left(\frac{1}{q_e}\right) t \tag{5}$$

where, k_1, k_2 and t are representing the equilibrium rate constants (1/min) and kinetic rate constant (g/min/mg), respectively. q_e and t are related to equilibrium adsorption capacity (mg/g) and time (min), respectively.

Langmuir, Freundlich, and Temkin isotherms were employed for isothermal studies. In Langmuir isotherm, there are some assumptions; (1) energy of the adsorption process is assumed to be uniform, (2) there is no interaction between adsorbate–adsorbate, and (3) the adsorption process is monolayer [25]. Langmuir isotherm model is expressed as below [25].

$$q_e = \frac{q_m k_L C_e}{1 + k_L C_e} \tag{6}$$

here, k_L refers to Langmuir constant (L/mg) elucidating the adsorption energy. qe and qm reveals equilibrium and maximum adsorption capacities (mg/g), respectively. Ce is in the relation with adsorbate concentration (mg/L) under the equilibrium conditions. Langmuir equation can be linearized as follows.

$$\frac{C_e}{q_e} = \frac{1}{K_L q_m} + \frac{C_e}{q_m} \tag{7}$$

Freundlich isotherm model is defined using Eq. (8).

$$q_e = k_F C_e^{\frac{1}{n}} \tag{8}$$

here, k_F and n indicate the adsorption and intensity capacity, respectively. The equation can be linearized as follows.

$$lnq_e = lnk_F + \frac{1}{n} lnC_e \tag{9}$$

Temkin isotherm model is defined utilizing Eq. (10) [26].

$$q_e = \frac{RT}{b_T} ln(AC_e) \tag{10}$$

here, T and R display temperature (K) and gas constant (J/mol.K), respectively. A and b_T refer to Temkin constant (L/mg) and the adsorption heat (J/mol), respectively. The relevant equation can be linearized as follows.

$$q_e = Bln(A) + BlnC_e \tag{11}$$

$$B = \frac{RT}{b_T}$$

2.7. Dynamic studies

The dynamic studies implying to fixed-bed column experiments were conducted in a glass cylindrical tube. Internal diameter and total height of the glass cylindrical tube was measured to be 1.1 cm and 30 cm, respectively. The optimal AC at various bed heights was packed in the glass cylindrical tube between two plugs of cotton supported by glass beads (Fig. 1).

The studied variables in this section were defined to be bed heights (1.5, 3, 4.5 cm) and solution flow rates (5, 10 and 15 mL/min). Upon dynamic studies, the effluent from the selected airlift dual internal circulation A2O bioreactor without changing the pH (6.5–7) was continuously fed to the adsorption column as upward flow with the aid of a peristaltic pump under room temperature. The sample was taken from various sampling sites for each bed height at pre-determined time intervals and analyzed as protein and carbohydrate contents. The behavior of the fixed-bed column over dynamic adsorption process using the secondary effluent containing protein and carbohydrate as a real adsorbate under optimum experimental conditions was examined by breakthrough (BT) curves. The total adsorbed solute mass (q_{total}, mg) can be obtained by measuring the area underbeneth the breakthrough plot via integrating the plot considering a given adsorbate concentration and flow rate (Q) employing the equation below.

$$q_{total} = \frac{Q}{1000} \int_{t=0}^{t=t_{total}} C_{ad}\, dt \tag{12}$$

where, Q and C_{ad} are defined as the flow rate (mL/min) and the adsorbed solute concentration (C_0-C_t) at the end of the total flow time till exhaustion time (t_{total}, min), respectively. The adsorption capacity in the activated carbon bed (q_{bed}, mg/g) was determined using the equation below.

$$q_{bed} = \frac{q_{total}}{w} \tag{13}$$

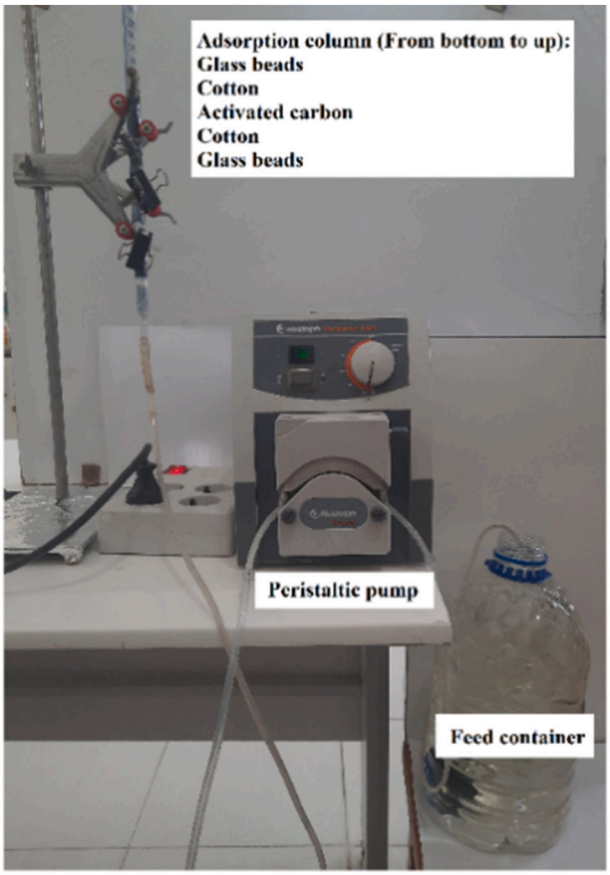

Fig. 1. A picture of the adsorption column.

where, q_{total} and w refer to the total adsorbed solute mass (mg) and adsorbent dosage used for each bed height (g), respectively. The total adsorbate mass (m_{total}, g) passed through the adsorption column and the adsorbate removal percentage (R, %) can be measured by the following equations using the parameters defined already.

$$m_{total} = \frac{C_0 Qt_{total}}{1000} \tag{14}$$

$$R = \frac{q_{total}}{m_{total}} \times 100 \tag{15}$$

3. Results and discussion

3.1. Characterization of the bituminous-based coal

The characteristics of the raw and modified bitumen precursors (acid-treated and pre-oxidation) are tabulated in Table 1. In general, the pre-treatment of the raw precursor with acid (HCl and HF) led to the reduction of the ash contents while the pre-oxidation process enhanced

Table 1
The results of proximate analysis obtained for the raw and modified bitumen.

Type of modification/proximate analysis (wt%)	Moisture	Ash	Volatile matter	Fixed carbon
Raw precursor	0.83	10.76	59.09	29.32
Pre-oxidized precursor	3.05	10.62	37.58	48.74
Acid treated precursor	0.82	0.81	67.13	31.24
Treatment with acid then oxidation	2.17	1.56	36.19	60.08
Oxidation then treatment with acid	1.8	0	47.78	50.42

the fixed carbon contents. From the Table, the precursor firstly pre-oxidized under heat then treated with acid showed the remarkable reduction in the ash context, and the increase in the fixed carbon compared to the others, therefore, it was considered for further studies.

3.2. Characterization of the synthesized ACs

The temperature behavior of the raw bituminous-based coal was investigated using TGA analysis (Fig. 2). From the Figure, an increment in temperature led to a two-step weight loss. Based on other reports, over carbonization process, moisture and volatile lumps were removed from the body of raw precursor [27]. The sharp peak observed from the Figure was ascribed to volatile evolution due to the presence of tar probably known as predominant product of devolatilization process.

The surface morphological features of the prepared ACs are denoted in the Fig. 3. Clearly from the Figure, the surface appearance of the KOH impregnated ACs was approximately intact that might be owing to the strong interaction of the KOH with pre-modified bitumen precursor [28,29]. However, in high impregnation ratio (3:1), some small pits were observed on the surface of the AC attributed to the carbon gasification [27].

The FTIR results of the prepared ACs are indicated in Fig. 4. Obviously, the FTIR spectra were similar for all the ACs. The wide peak of around 3500 cm^{-1} was assigned to the stretching vibration of OH. The peaks of around 2857 and 2949 cm^{-1} were ascribed to the asymmetric stretching vibration of C—H bond [28]. Peak appeared at 1726 cm^{-1} belongs to C═O stretching vibration [30]. The peak of 1630.21 cm^{-1} was related to the existence of the adsorbed H_2O molecules [31]. Sharp peak of 1089 cm^{-1} was attributed to C—O—C stretching vibration of ethers [30]. The peaks appeared below 900 nm are assigned to the stretching vibration of C—H and C—C [32].

The textural features of the prepared ACs are including specific surface area (determined by BET method (S_{BET})), microporosity volume (V_{mic}), mesoporrosity volume (V_{mes}), total volume (V_{total}), pore diameter (R_p) and yield. The obtained results are given in Table 2. Evidently, all the prepared activated carbons showed the improved textural properties compared to the commercial activated carbon (CAC). The increase in impregnation ratio up to 2:1 led to the increment in S_{BET} owing to the enhancement in microporosity. According to Heidari et al., the usage of KOH as activator brought into the considerable increment in the S_{BET} due to the formation of micro- and sub-microporosity over carbonization process [33]. In overall, substantial factors like the S_{BET}, type and amount of pore volume influence on the uptake of the various contaminations by the activated carbon-coupled adsorption processes. Based on the results, rising the impregnation ratio to 3:1 (activator to precursor mass ratio) gave rise to the reduction in S_{BET} due to the development of mesoporosity. Such statements were come up by Heidari et al. using impregnation ratio of 2.5 as $ZnCl_2$ to eucalyptus mass ratio [33]. In addition, by increasing impregnation ratio, the produced activated carbon yield was decreased.

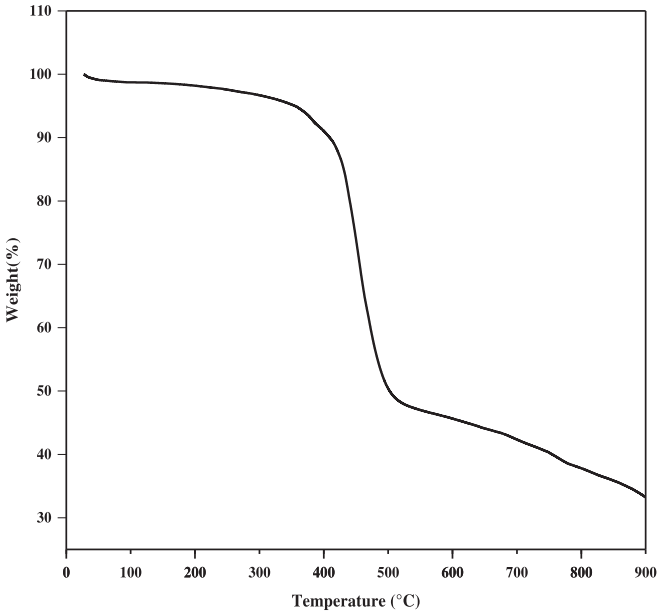

Fig. 2. TGA analysis of the raw bitumen precursor.

3.3. Performance of the prepared activated carbons in batch experiments

This section includes two main stages, in the first stage, the optimum AC was selected among the various activated carbons impregnated with different ratios of KOH and bitumen i.e. 1:1, 2:1 and 3:1 using three adsorbates of MB, BSA and dextrose. In the second stage, the impact of the influential variables such as the AC dosage, initial adsorbate concentration and contact time is checked on the performance of the optimum activated carbon to find the desired adsorption experimental conditions.

3.3.1. Determination of the optimum activated carbon

Based on the experimental conditions defined in the preceding paragraphs, the KOH-2 impregnated activated carbon was chosen as the optimum activated carbon on the basis of the highest adsorption capacity and pollutant removal as MB, BSA and dextrose. In general, although the KOH-3 impregnated activated carbon showed a litter better performance over 2:1 ratio, in order not to consume a significant dosage of activator, the 2:1 ratio was chosen as an optimal ratio. The improvement in MB, BSA and dextrose removal was in association with the enhanced mesoporosity and microporosity. It should be mentioned the activated carbons prepared from chemical activator of KOH were selected as optimum adsorbents among other activated carbons produced by chemical activators of K_2CO_3 and H_3PO_4 over preliminary studies conducted using 600 mg/L of MB and 0.2 g/L of each adsorbent dosage for contact time of 3 h (obtained data are not presented here). The obtained findings are presented in Table 3.

3.3.2. The effect of the AC dosage

Note that in this study, the adsorption study was conducted at 200 rpm agitation speed and room temperature. The KOH-2 impregnated AC dosage was optimized at constant initial concentration of MB (600 mg/L), BSA (200 mg/L) and dextrose (200 mg/L). The range of the studied AC dosage was 0.1–1, 0.2–1.0 and 0.5–1.5 g/L for MB, BSA and dextrose, respectively. Fig. 5 reveals the influence of the activated carbon dosage on the adsorption capacity and removal percentage using MB. From the Figure, the optimum AC with 0.2 g/L showed the best behavior as mentioned responses due to presence of vacant sorption surface sites and adequate driving force. After this point, the dye removal was not changed remarkably, while, the adsorption capacity reduced sharply owing to reduced driving force in the mass transfer that stem from decreased concentration gradient. To get the exact mass of the adsorbent, the AC dosage was narrowed into two amounts i.e. 0.21 and 0.22 g/L. According to the Fig. 5, the 0.22 g/L value was optimal as a result of high adsorption capacity and dye removal efficiency. From the Fig. 6, it was found that the rise in the activated carbon dosage up to 0.6 and 1 g/L resulted in the considerable elimination and reasonable uptake capacity using BSA and dextrose adsorbates, respectively. However, narrowing adsorbent dosage for both adsorbates showed no significant impact on the relevant responses. Therefore, 0.6 and 1 g/L was selected as the optimum value for BSA and dextrose adsorbates, respectively. In this study, considering in the first stage of this part (determination of optimum activated carbon), the functionality of the AC for the dextrose adsorbate was not as high as the BSA, so, the higher range of the adsorbent dosage was taken account (0.5, 1 and 1.5 g/L). In general, optimization of activated carbon dosage was done based on two

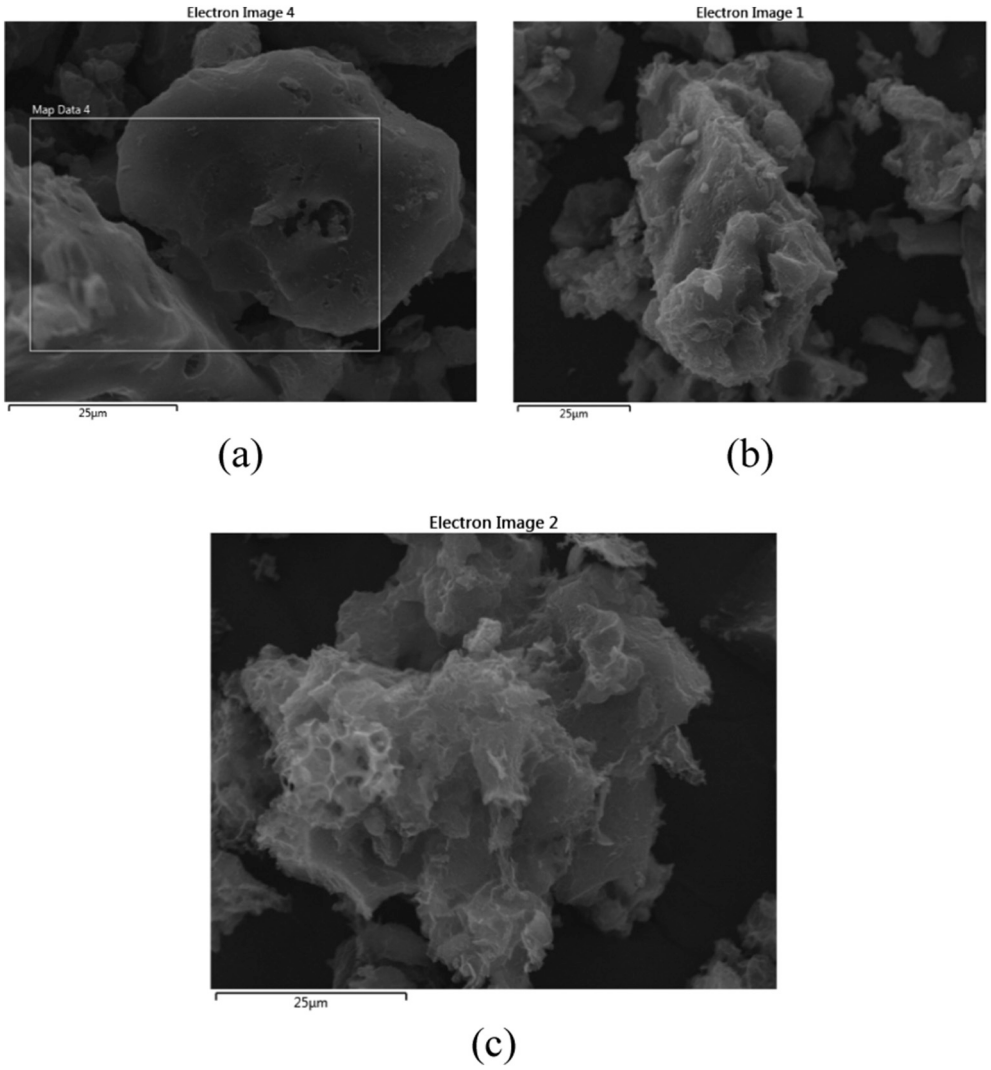

Fig. 3. The SEM images of ACs chemically prepared using modified bitumen precursor and KOH at three impregnation ratios of (a) 1:1, (b) 2:1 and (c) 3:1.

substantial factors; reaching the best performance along with saving adsorbent dosage.

3.3.3. *The impact of the initial adsorbate concentration*

The function of KOH-2 impregnated AC was assessed at various initial concentrations using three adsorbates (i.e. MB; 300–1000 mg/L, BSA and dextrose each with 100–300 mg/L) as indicated in Fig. 7. The experiments were carried out using optimum amounts of adsorbent dosage obtained for each adsorbate at agitation speed of 200 rpm under ambient temperature. From the Figure, a drastic increment in the adsorption capacity for three adsorbates was found by increasing the adsorbate concentration at the initial stage. The increase in concentration gradient leading to the improvement in the driving force and mitigation in the mass transfer resistance justified these results. Whereas, the sorption active sites facing high pollutant concentrations were occupied leading to the reduction in the dye removal. The initial concentrations of 600, 200, and 200 mg/L were found as optimal values for the MB, BSA and dextrose, respectively. Kumar et al., concluded the pollutant removal as MB and phenol decreased from 99.95 to 77.49 % and 99.19 to 75.37 %, respectively, at 100–500 mg/L [5]. The equilibrium adsorption capacity of 249.88–968.74 mg/g and 19.84–75.37 mg/g was achieved at 100–500 mg/L for MB and phenol, respectively.

3.3.4. *The impact of contact time*

The function of the optimum KOH-2 impregnated AC in adsorption of three various adsorbates was evaluated at various contact times to reach the equilibrium time. The achieved findings are exhibited in Fig. S1. Clearly, a remarked increase in the adsorption capacity and pollutant removal efficiency were obtained at the first time of the adsorption process. Then, the relevant responses were increased in a slow speed by passing time due to the reduction in the concentration gradient as driving force and occupation of sorption active sites on the AC surface, leading to the reduction in the mass transfer phenomenon [4]. This growing trend would slowly continue until reaching the equilibrium state, then stop. This statement was supported by literature [4,5,34].

The outcomes of this study showed that the adsorption intensity related to the equilibrium time was less than results reported by Kumar et al. where the authors could reach the equilibrium time within the first 10 min, 60 min and 60 min for MB with the concentration of 100 and 500 mg/L, and any concentration of phenol (100–500 mg/L), respectively [5]. From the Figure, the equilibrium time was obtained at 220 min, 180 min and 196 min for MB, BSA and dextrose with initial concentrations of 600, 200 and 200 mg/L, respectively. The adsorption capacity and pollutant removal efficiency as MB, BSA and dextrose were gained to be 2711 mg/g and 99.4 %, 283 mg/g and 84.9 %, and 164 mg/g and 82 %, respectively, at relevant equilibrium time. The functionality of the KOH-2 impregnated AC recognized as the selected one and

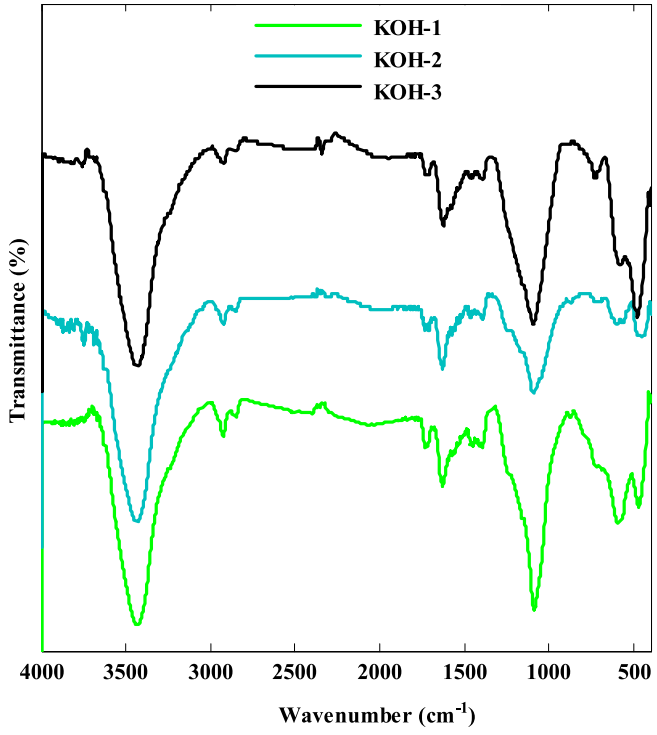

Fig. 4. The FTIR spectra obtained for the activated carbons impregnated with KOH at ratios of 1:1, 2:1 and 3:1.

Table 2
Textural parameters of prepared ACs.

Sample	Yield, %	Textural parameters					
		BET, m^2/g	V_{mic}, cm^3/g	V_{mes}, cm^3/g	V_{tot}, cm^3/g	R_{mic}, nm	V_{mic}/V_{tot}, %
KOH-1	20.7	1093.1	0.50	0.22	0.62	2.29	80.4
KOH-2	12.4	1420.8	0.75	0.42	0.93	2.61	80.73
KOH-3	6.7	1387.8	0.78	0.62	0.97	2.78	80.26
CAC	–	907.6	0.42	0.06	0.48	0.37	86.54

Table 3
The experimental data obtained from screening various activated carbons using different adsorbates over batch tests.

Type of AC	Dye removal	q, mg/g
MB: 600 mg/L, adsorbent dosage: 0.2 g/L, agitation speed: 200 rpm, contact time: 3 h		
KOH-1	63.6	1908.3
KOH-2	92.4	2772.5
KOH-3	94.8	2844.4
BSA: 200 mg/L, adsorbent dosage: 0.5 g/L, agitation speed: 200 rpm, contact time: 3 h		
KOH-1	60.6	242.4
KOH-2	78.0	312
KOH-3	80	320
Dextrose: 200 mg/L; adsorbent dosage: 0.5 g/L, agitation speed: 200 rpm, contact time: 3 h		
KOH-1	30.5	122
KOH-2	50.1	200.4
KOH-3	55.1	220.4

commercial activated carbon (CAC) was compared under optimum conditions. The obtained findings are given in Table S1. From the results, the selected AC denoted the superior function upon adsorption of MB, BSA and dextrose over CAC. Vakili et al. reported maximum

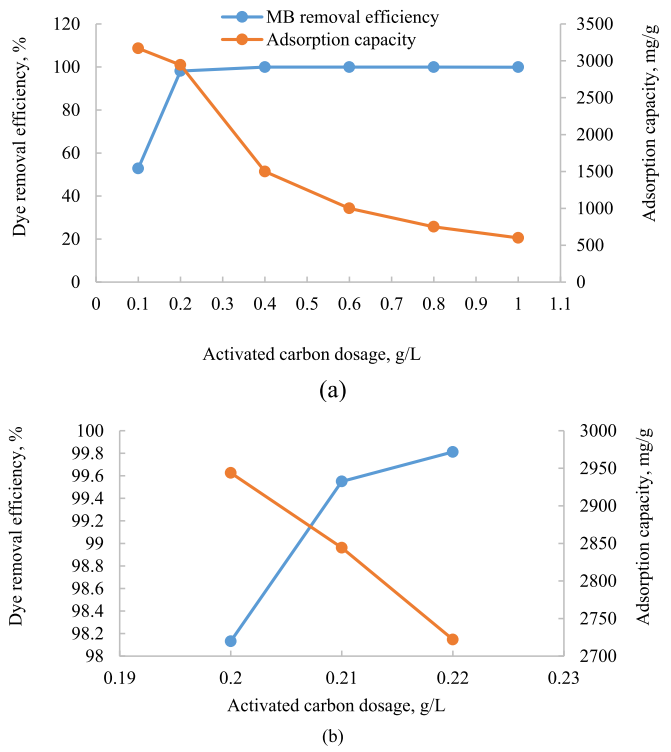

Fig. 5. The adsorption capacity and MB removal efficiency of KOH-2 impregnated AC at various adsorbent dosages (a) 0.1–1 g/L, and (b) 0.2–0.22 g/L (initial MB concentration of 600 mg/L and contact time of 3 h).

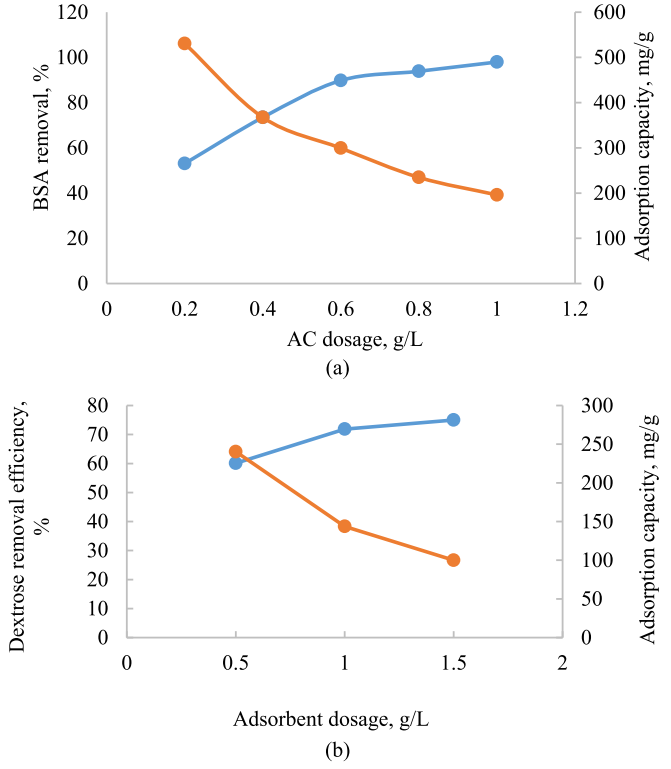

Fig. 6. The adsorption capacity and removal efficiency of KOH-2 impregnated AC at various adsorbent dosages using (a) BSA and (b) dextrose (initial concentration of 200 mg/L for each adsorbate and contact time of 3 h).

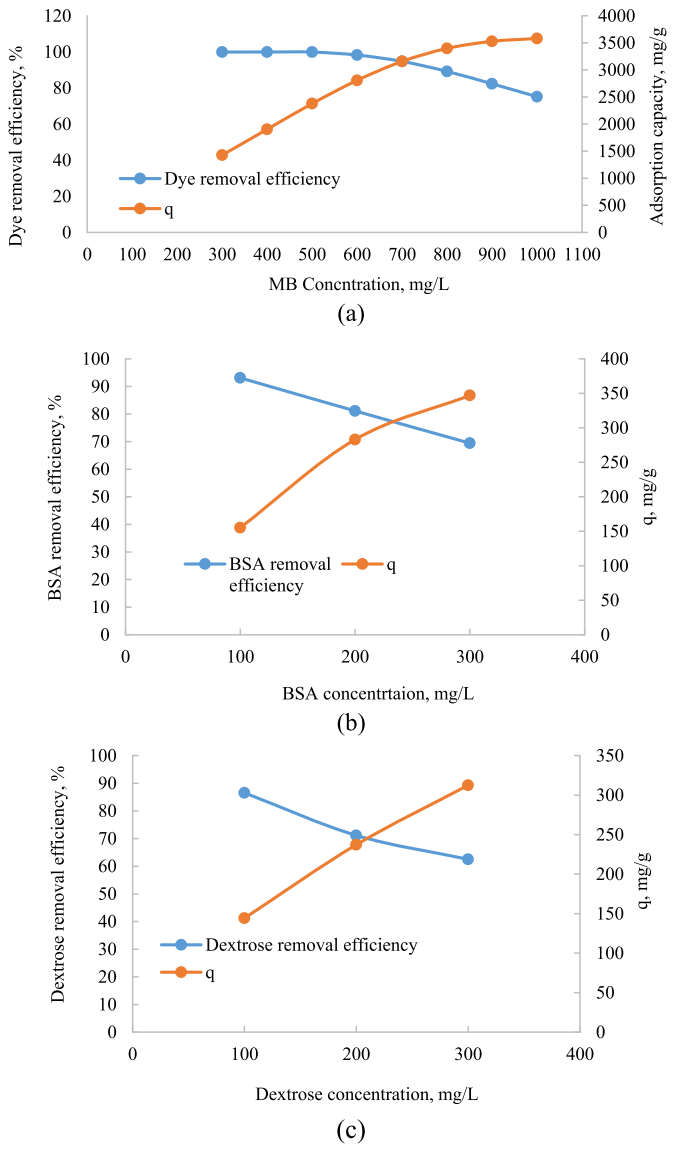

Fig. 7. The adsorption capacity and pollutant removal efficiency of the KOH-2 impregnated AC using (a) MB, (b) BSA, and (c) dextrose (at 0.22, 0.6 and 1 g/L for MB, BSA and dextrose, respectively, at contact time of 3 h).

adsorption capacity of 307.4 mg/g with 400 mg/L MB using physically synthesized walnut shell-based AC [4]. In another study, the maximum adsorption capacity of 968.74 mg/g and 75.37 mg/g for 500 mg/L of MB and phenol, respectively, was reported [5].

3.4. Kinetic studies

In order to describe the solute adsorption rate and control the residence time of adsorbate at the activated carbon-adsorbate solution interface, the kinetic studies were carried out. Results of pseudo-first order, pseudo-second-order and intraparticle diffusion along with kinetic parameters for three adsorbates (MB, BSA and dextrose) onto the optimum KOH-2 impregnated AC are displayed in Figs. S2 and S3, and Table S2. From the Figures and Table, the similar trend was observed in kinetic models all the studied adsorbates. The experimental data showed the upmost fitness with pseudo-second order model with the highest R^2 of 1, 0.9816 and 0.9835 for the MB, BSA and dextrose, respectively. In addition, in pseudo-second order model, theoretical value of (q_c) was similar to the experimental value (q_e). From the literature, the more fitness of the experimental data with the pseudo-second-order confirms the chemisorption mechanism that is the rate-limiting step, resulting in stronger binding and higher removal efficiency [2,35–37]. The chemisorption process involves the sharing of electrons and the formation of valence forces [4]. The fit with the pseudo-second-order model suggests that the adsorption rate is governed by the adsorption sites on activated carbon [38]. Further, intraparticle diffusion model was employed to verify the intraparticle diffusion mechanism for three studied adsorbates with the linear plots and high R^2, showing intraparticle diffusion model has an important contribution in the adsorption process [4]. Moreover, the high values of the rate constant in the intraparticle diffusion model can serve as evidence of strong adsorptive interactions between the adsorbate and the adsorbent [4]. According to the literature, if the C value in the intraparticle diffusion model is zero, the adsorption process rate is entirely controlled by intraparticle diffusion [4]. In this study, the C values were greater than zero, which is consistent with findings reported in the literature [4,5,37]. This result indicates that the intraparticle diffusion model is not the sole rate-limiting step [37,38]. The kinetic findings were in a good consistence with outcomes obtained by Kumar et al. who used MB and phenol as adsorbate [5]. The kinetic study is vital for designing and optimizing the adsorption process, as it helps determine the contact time and adsorption rate under varying conditions [35,36]. From the Table, the rate constants showed good agreement with the values reported in the literature [4].

3.5. Isotherm studies

At equilibrium conditions, the isotherm studies help describe how the adsorbed solutes are distributed between solid phase (activated carbon) and liquid phase (adsorbate solution). The results of the experimental data fitting with isotherm models i.e. Langmuir, Frundlich and Tempkin along with isotherm parameters for three adsorbates are revealed in Fig. S4 and Table S3. In overall, the validation of the isotherm models was confirmed by linear plots. The fitness degree of the experimental data with the employed isotherm models were estimated by R^2 values. From the Table, the adaptation level of various isotherm models for the three adsorbates in terms of the increase in R^2 values is in the order of Langmuir >Tempkin > Freundlich. A comparable trend was noted in the literature, where methylene blue (MB) and phenol served as adsorbates, utilizing walnut-based activated carbon (physically synthesized) and fox nutshell-based activated carbon (chemically synthesized) [4,5].

3.6. Continuous studies

3.6.1. The impact of the AC bed height

The effect of the AC bed height on the breakthrough curves for protein and carbohydrate adsorbates known as main constituents of soluble microbial products (SMP) from selected bioreactor's effluent (the hybrid dual circulation airlift A2O (DCAL-A2O) bioreactor) at constant flow rate is displayed in Fig. S5. Evidently, both the breakthrough and exhaustion time were lengthened by increasing the bed height. According to Kumar et al., the rise in the breakthrough time with the bed height could be in relation with the increase in the distance [5]. In this condition, the mass transfer zone is considered to move from the entry point of the adsorption column bed to the outlet [5]. The enhanced adsorption capacity for both adsorbates (protein and carbohydrate) with the increment in the bed height was ascribed to the large specific surface area of the AC and enhanced sorption active sites [5]. Furthermore, at exhaustion time, the increase in the AC mass corresponded with the rise in the bed height resulted in the increment in the treated volume of the biologically treated wastewater per unit mass of the AC. The results gained are presented in Table S4. Based on the obtained outcomes, 4.5 cm was considered as optimum bed height for further experiments.

3.7. The impact of the feed flow rate

The adsorption behavior of optimum KOH-2 impregnated AC was assessed under the varied feed flow rates and optimal bed height of 4.5 cm using the effluent from the hybrid ALDC-A2O bioreactor treating the milk processing wastewater (MPW). The obtained experimental data were processed and denoted as the breakthrough curves in Fig. S6. Obviously, from the Figure, the increase in the flow rate was impacted on the adsorption function negatively via the mitigation in the breakthrough and exhaustion time as well as the reduction in the adsorbate removal. The reason behind such observations was ascribed to lack of the sufficient residence time for diffusing the adsorbate into the internal AC-based adsorbent pores [5,39,40].

As a conclusion, adsorption column revealed the best performance under optimum experimental conditions achieved at the bed height and the feed flow rate of 4.5 cm and of 5 mL/min, respectively.

Performance investigation of the selected AC as post-treatment of biologically treated milk processing wastewater and comparative study with literature were discussed in supplementary file.

4. Conclusions

In this research, the bituminous-based ACs were chemically synthesized using various activators i.e. KOH, K_2CO_3 and H_3PO_4 with impregnation ratios of 1:1, 2:1 and 3:1. From the screening studies performed over the batch experiments, the KOH-2 impregnated activated carbon was chosen as the optimum adsorbent. According to the obtained results, the chosen AC gained the highest adsorption capacity of 2710.6, 283, and 273 mg/g adsorbing MB, BSA and dextrose, respectively. In the following, the fixed-bed column studies were conducted using the optimum activated carbon under varied experimental conditions as bed height and flow rate to remove the residual organic matters from the hybrid dual internal circulation airlift A2O (DCAL-A2O) bioreactor's effluent treating milk processing wastewater. Based on the findings, the chosen AC showed the best performance at the bed height of 4.5 cm and flow rate of 5 min/ml with the highest breakthrough time of 480 and 380 min for the protein and carbohydrate, respectively. The adsorption column reduced successfully the residual organic matters contents from 35 mg-TOC/L to 6.6 mg-TOC/L as well as the significant mitigation in the microbial burden. Totally, utilizing low-cost waste materials like bitumen as precursors enhances economic feasibility by transforming industrial waste into valuable resources, promoting sustainability, and reducing raw material costs. However, to advance the application of bitumen-based activated carbon (AC), an economic evaluation is necessary and will be addressed in future work.

CRediT authorship contribution statement

Zahra Rahimi: Writing – original draft, Methodology, Investigation, Conceptualization. **Ali Akbar Zinatizadeh:** Writing – review & editing, Supervision, Methodology. **Sirus Zinadini:** Writing – review & editing. **Habibollah Younesi:** Writing – review & editing, Methodology. **Mark van Loosdrecht:** Writing – review & editing. **Shohreh Azizi:** Funding acquisition, Validation, Writing – review & editing.

Declaration of competing interest

The authors declare that they have no known competing financial interests or personal relationships that could have appeared to influence the work reported in this paper.

Acknowledgments

The authors wish to thank Water, Soil, Erosion, and Drought Headquarter, Iran, and Razi University, Iran, for financially supporting and providing lab facilities for this study. The authors are also grateful to the SASOL National Research Foundation of South Africa (SASOL-NRF) University Collaborative Research Grants (Grant No. 138626) for their support.

Appendix A. Supplementary data

Supplementary data to this article can be found online at https://doi.org/10.1016/j.jwpe.2025.107015.

Data availability

Data will be made available on request.

References

[1] H. Sayğili, F. Güzel, High surface area mesoporous activated carbon from tomato processing solid waste by zinc chloride activation: process optimization, characterization and dyes adsorption, J. Clean. Prod. 113 (2016) 995–1004, https://doi.org/10.1016/j.jclepro.2015.12.055.

[2] A.A.E.A. Elfiky, M.F. Mubarak, M. Keshawy, I.E.T. El Sayed, T.A. Moghny, Novel nanofiltration membrane modified by metal oxide nanocomposite for dyes removal from wastewater, Environ. Dev. Sustain. 26 (2024) 19935–19957, https://doi.org/10.1007/s10668-023-03444-1.

[3] H. Zangeneh, M. Farhadian, A.A. Zinatizadeh, N (urea) and CN (L-asparagine) doped TiO_2-CuO nanocomposites: fabrication, characterization and photodegradation of direct red 16, J. Environ. Chem. Eng. 8 (1) (2020) 103639, https://doi.org/10.1016/j.jece.2019.103639.

[4] A. Vakili, A.A. Zinatizadeh, Z. Rahimi, S. Zinadini, P. Mohammadi, S. Azizi, A. Karami, M. Abdulgader, The impact of activation temperature and time on the characteristics and performance of agricultural waste-based activated carbons for removing dye and residual COD from wastewater, J. Clean. Prod. 382 (2023) 134899, https://doi.org/10.1016/j.jclepro.2022.134899.

[5] A. Kumar, H.M. Jena, Removal of methylene blue and phenol onto prepared activated carbon from Fox nutshell by chemical activation in batch and fixed-bed column, J. Clean. Prod. 137 (2016) 1246–1259, https://doi.org/10.1016/j.jclepro.2016.07.177.

[6] W. Chen, R. Parette, J. Zou, F.S. Cannon, B.A. Dempsey, Arsenic removal by iron-modified activated carbon, Water Res. 41 (2007) 1851–1858, https://doi.org/10.1016/j.watres.2007.01.052.

[7] S. Hong, F.S. Cannon, P. Hou, T. Byrne, C. Nieto-Delgado, Sulfate removal from acid mine drainage using polypyrrole-grafted granular activated carbon, Carbon N. Y. 73 (2014) 51–60, https://doi.org/10.1016/j.carbon.2014.02.036.

[8] F. Kaouah, S. Boumaza, T. Berrama, M. Trari, Z. Bendjama, Preparation and characterization of activated carbon from wild olive cores (oleaster) by H_3PO_4 for the removal of Basic Red 46, J. Clean. Prod. 54 (2013) 296–306, https://doi.org/10.1016/j.jclepro.2013.04.038.

[9] H. Xue, X. Wang, Q. Xu, F. Dhaouadi, L. Sellaoui, M.K. Seliem, A. Ben Lamine, H. Belmabrouk, A. Bajahzar, A. Bonilla-Petriciolet, Z. Li, Q. Li, Adsorption of methylene blue from aqueous solution on activated carbons and composite prepared from an agricultural waste biomass: a comparative study by experimental and advanced modeling analysis, Chem. Eng. J. 430 (2022), https://doi.org/10.1016/j.cej.2021.132801.

[10] A.M. Redding, F.S. Cannon, The role of mesopores in MTBE removal withgranular activated carbon, Water Res. 56 (2014) 214–224, https://doi.org/10.1016/j.watres.2014.02.054.

[11] R.M. Novais, A.P.F. Caetano, M.P. Seabra, J.A. Labrincha, R.C. Pullar, Extremely fast and efficient methylene blue adsorption using eco-friendly cork and paper waste-based activated carbon adsorbents, J. Clean. Prod. 197 (2018) 1137–1147, https://doi.org/10.1016/j.jclepro.2018.06.278.

[12] H. Wang, Z. Li, S. Yahyaoui, H. Hanafy, M.K. Seliem, A. Bonilla-Petriciolet, G. Luiz Dotto, L. Sellaoui, Q. Li, Effective adsorption of dyes on an activated carbon prepared from carboxymethyl cellulose: experiments, characterization and advanced modelling, Chem. Eng. J. 417 (2021), https://doi.org/10.1016/j.cej.2020.128116.

[13] R. Sandoval, A.M. Cooper, K. Aymar, A. Jain, K. Hristovski, Removal of arsenic and methylene blue from water by granular activated carbon media impregnated with zirconium dioxide nanoparticles, J. Hazard. Mater. 193 (2011) 296–303, https://doi.org/10.1016/j.jhazmat.2011.07.061.

[14] A.K. El-Sawaf, A.A. Nassar, A.A. El Aziz Elfiky, M.F. Mubarak, Advanced microcrystalline nanocellulose-based nanofiltration membranes for the efficient treatment of wastewater contaminated with cationic dyes, Polym. Bull. 81 (2024) 12451–12476, https://doi.org/10.1007/s00289-024-05279-w.

[15] Z. Rahimi, A.A. Zinatizadeh, S. Zinadini, M. van Loosdrecht, D.J. Batstone, A high-rate A2O bioreactor with airlift-driven circulation and anoxic hybrid growth for enhanced carbon and nutrient removal from a nutrient rich wastewater, Chemosphere 370 (2025) 143811, https://doi.org/10.1016/J.CHEMOSPHERE.2024.143811.

[16] T. Kopac, Y. Kırca, A. Toprak, Synthesis and characterization of KOH/boron modified activated carbons from coal and their hydrogen sorption characteristics, Int. J. Hydrog. Energy 42 (2017) 23606–23616, https://doi.org/10.1016/j.ijhydene.2017.01.195.

[17] N. Janga, X. Ren, G. Kim, C. Ahn, J. Cho, I.S. Kim, Characteristics of soluble microbial products and extracellular polymeric substances in the membrane bioreactor for water reuse, Desalination 202 (2007) 90–98, https://doi.org/10.1016/j.desal.2005.12.043.
[18] O.H. Lowry, N.J. Rosebrough, A.L. Farr, R.J. Randall, Protein measurement with the Folin phenol reagent, J. Biol. Chem. 193 (1951) 265–275, https://doi.org/10.1016/s0021-9258(19)52451-6.
[19] M. Dubois, K.A. Gilles, J.K. Hamilton, P.A. Rebers, F. Smith, Colorimetric method for determination of sugars and related substances, Anal. Chem. 28 (1956) 350–356, https://doi.org/10.1021/ac60111a017.
[20] A.K. El-Sawaf, S.R. El-Dakkony, M.A. Zayed, A.M. Eldesoky, A.A. Nassar, A. El Shahawy, M.F. Mubarak, Green synthesis and characterization of magnetic gamma alumina nanoparticlesfor copper ions adsorption from synthetic wastewater, Results Eng. 22 (2024) 101971, https://doi.org/10.1016/j.rineng.2024.101971.
[21] T. Calvete, E.C. Lima, N.F. Cardoso, J.C.P. Vaghetti, S.L.P. Dias, F.A. Pavan, Application of carbon adsorbents prepared from Brazilian-pine fruit shell for the removal of reactive orange 16 from aqueous solution: kinetic, equilibrium, and thermodynamic studies, J. Environ. Manag. 91 (2010) 1695–1706, https://doi.org/10.1016/j.jenvman.2010.03.013.
[22] B.H. Hameed, A.A. Rahman, Removal of phenol from aqueous solutions by adsorption onto activated carbon prepared from biomass material, J. Hazard. Mater. 160 (2008) 576–581, https://doi.org/10.1016/j.jhazmat.2008.03.028.
[23] T. Budinova, E. Ekinci, F. Yardim, A. Grimm, E. Björnbom, V. Minkova, M. Goranova, Characterization and application of activated carbon produced by H3PO4 and water vapor activation, Fuel Process. Technol. 87 (2006) 899–905, https://doi.org/10.1016/j.fuproc.2006.06.005.
[24] Y.S. Ho, G. McKay, Pseudo-second order model for sorption processes, Process Biochem. 34 (1999) 451–465, https://doi.org/10.1016/S0032-9592(98)00112-5.
[25] I. Langmuir, The adsorption of gases on plane surfaces of glass, mica and platinum, J. Am. Chem. Soc. 40 (1918) 1361–1403, https://doi.org/10.1021/ja02242a004.
[26] V. Temkin, M.J. Pyzhev, Recent modifications to Langmuir isotherms, Acta Physiochim. 12 (12) (1940) 217. https://www.scienceopen.com/document?vid=ef69d115-706c-4007-b3ce-2f45e972f91b. (Accessed 16 September 2022).
[27] L.Y. Hsu, H. Teng, Influence of different chemical reagents on the preparation of activated carbons from bituminous coal, Fuel Process. Technol. 64 (2000) 155–166, https://doi.org/10.1016/S0378-3820(00)00071-0.
[28] M. Nowrouzi, H. Younesi, N. Bahramifar, High efficient carbon dioxide capture onto as-synthesized activated carbon by chemical activation of Persian Ironwood biomass and the economic pre-feasibility study for scale-up, J. Clean. Prod. 168 (2017) 499–509, https://doi.org/10.1016/j.jclepro.2017.09.080.
[29] D. Liu, J. Gao, Q. Cao, S. Wu, Y. Qin, Improvement of activated carbon from Jixi bituminous coal by air preoxidation, Energy Fuel 31 (2017) 1406–1415, https://doi.org/10.1021/acs.energyfuels.6b02875.
[30] J. Guo, A.C. Lua, Surface functional groups on oil-palm-shell adsorbents prepared by H_3PO_4 and KOH activation and their effects on adsorptive capacity, Chem. Eng. Res. Des. 81 (2003) 585–590, https://doi.org/10.1205/026387603765444537.
[31] M. Nowrouzi, H. Younesi, N. Bahramifar, Superior CO_2 capture performance on biomass-derived carbon/metal oxides nanocomposites from Persian ironwood by H_3PO_4 activation, Fuel 223 (2018) 99–114, https://doi.org/10.1016/j.fuel.2018.03.035.
[32] S. Timur, I.C. Kantarli, S. Onenc, J. Yanik, Characterization and application of activated carbon produced from oak cups pulp, J. Anal. Appl. Pyrolysis 89 (2010) 129–136, https://doi.org/10.1016/j.jaap.2010.07.002.
[33] A. Heidari, H. Younesi, A. Rashidi, A.A. Ghoreyshi, Adsorptive removal of CO_2 on highly microporous activated carbons prepared from *Eucalyptus camaldulensis* wood: effect of chemical activation, J. Taiwan Inst. Chem. Eng. 45 (2014) 579–588, https://doi.org/10.1016/j.jtice.2013.06.007.
[34] N.U.M. Nizam, M.M. Hanafiah, E. Mahmoudi, A.A. Halim, A.W. Mohammad, The removal of anionic and cationic dyes from an aqueous solution using biomass-based activated carbon, Sci. Rep. 11 (2021) 1–17.
[35] A.K. El-Sawaf, A.A. Nassar, A.A. El Aziz Elfiky, M.F. Mubarak, Advanced microcrystalline nanocellulose-based nanofiltration membranes for the efficient treatment of wastewater contaminated with cationic dyes, Polym. Bull. 81 (2024) 12451–12476, https://doi.org/10.1007/s00289-024-05279-w.
[36] A.H. Ragab, N.F. Gumaah, A.A. El Aziz Elfiky, M.F. Mubarak, Exploring the sustainable elimination of dye using cellulose nanofibrils- vinyl resin based nanofiltration membranes, BMC Chem. 18 (2024) 1–15, https://doi.org/10.1186/s13065-024-01211-5.
[37] S. Cheng, X. Zeng, P. Liu, One-step synthesis of magnetic N-doped carbon nanotubes derived from waste plastics for effective Cr(VI) removal, Arab. J. Chem. 17 (2024) 105956, https://doi.org/10.1016/J.ARABJC.2024.105956.
[38] X. Qin, S. Cheng, B. Xing, X.X. Qu, C. Shi, W. Meng, C. Zhang, H. Xia, Preparation of pyrolysis products by catalytic pyrolysis of poplar: application of biochar in antibiotic wastewater treatment, Chemosphere 338 (2023) 139519, https://doi.org/10.1016/j.chemosphere.2023.139519.
[39] C.R. Girish, V.R. Murty, Adsorption of phenol from aqueous solution using *Lantana camara*, forest waste: packed bed studies and prediction of breakthrough curves, Environ. Process. 2 (2015) 773–796, https://doi.org/10.1007/s40710-015-0117-z.
[40] N. Mohammed, N. Grishkewich, H.A. Waeijen, R.M. Berry, K.C. Tam, Continuous flow adsorption of methylene blue by cellulose nanocrystal-alginate hydrogel beads in fixed bed columns, Carbohydr. Polym. 136 (2016) 1194–1202, https://doi.org/10.1016/j.carbpol.2015.09.099.